JOURNAL OF
Materials
CHEMISTRY

Rh, Ru and Ir catalysts obtained by HT precursors: effect of the thermal evolution and composition on the material structure and use†

Francesco Basile,*[a] Giuseppe Fornasari,[a] Massimo Gazzano[b] and Angelo Vaccari[a]

[a]*Dipartimento di Chimica Industriale e dei Materiali, Univesita' di Bologna, Viale Risorgimento 4, 40136 Bologna, Italy. E-mail: basile@ms.fci.unibo.it*
[b]*Istituto per la Sintesi Organica e la Fotoreattività, CNR, Via Selmi 2, 40126 Bologna, Italy*

Received 28th May 2002, Accepted 25th June 2002
First published as an Advance Article on the web 3rd October 2002

The crystal structure refinements of six M/Mg/Al mixed oxides containing cations in the ratio M : Mg : Al = 5 : 71 : 24 (where M is Ru, Rh or Ir) have been carried out using both neutron and X-ray powder full pattern diffraction analysis. The samples were obtained by thermal decomposition of hydrotalcite-type anionic clays at 923 or 1173 K. MgO-type and spinel-type oxides were detected along with IrO_2 or RuO_2. Because of the presence of crystal defects, a more flexible spinel-like structure was used to fit the MgO-type phase, too. The three elements that were investigated exhibit different solubilities in the various oxide lattices but invariably substitute in the 16d site of the spinel structure. The variation of the Mg : Al ratio was utilised to change the distribution of the Rh and Ru in the present phases. The Mg : Al ratio affects significantly the structure and the distribution of the noble metal in the calcined material. The activity in the partial oxidation of methane carried out after reduction has changed as a function of the Mg : Al ratio and has been found to be higher at high Mg : Al ratios.

Introduction

The hydrotalcite-like materials have been widely studied to prepare catalysts used in several industrial reactions. The thermal decomposition through calcination of hydrotalcite-type (HT) anionic clays having the general formula $[M(\textsc{ii})_{1-x}M(\textsc{iii})_x(OH)_2]^{x+}[A^{n-}{}_{x/n}]^{x-}\cdot mH_2O$ [where M is a metal cation and A an anion (usually carbonate)] is a well known method of preparing homogeneous mixed oxides characterised by the intimate mixing of components.[1–3] This method has recently been applied in the preparation of catalysts containing well dispersed noble metal atoms which, after reduction, form stabilised nanoparticles that have numerous applications (in the liquid or gaseous phases) in many reactions of scientific and industrial interest.[4,5] In particular, the preparation of the noble metal-containing hydrotalcite tries to overcome the problems related to the stability of the metal particles in severe reaction conditions[5] by developing a strong interaction with the support. The noble metal-containing catalysts are usually prepared by wetness impregnation of different supports,[6] but the interaction with the support is often weak. These properties are particularly interesting for the reaction of the partial oxidation of methane at very low residence times since the catalyst can reach very high temperatures.[7,8] This process has a wide scientific and industrial interest since it is hypothesised to be an interesting alternative to the steam reforming process for the production of synthesis gas or hydrogen. Moreover, the synthesis from HT precursors may overcome the problems of reproducibility and of homogeneous distribution of the noble metals as the cations are uniformly distributed inside the brucite-type sheet of the HT structure.[9] The thermal evolution of new Rh, Ru, Ir, Pd, Pt catalysts has been reported recently.[10] It was noted that the thermal decomposition of these catalysts led to the formation of phases characterised by defective structures. There is a need, therefore, to carry out further studies on these systems with a view to ascertaining the relationship between structure and reactivity.

Previous studies have demonstrated that although mixed oxides obtained from magnesium-containing HT precursors show diffraction patterns similar to those of MgO-type phases, their lattices are far from an ideal 'rock-salt' phase as they resemble a defective, spinel-like structure.[11–13] The determination of the location of the ions in these phases is essential in order to establish the role of the noble metal.

This paper discusses the structural insights gleaned from neutron and X-ray diffraction studies of M/Mg/Al mixed oxides (M : Mg : Al = 5 : 71 : 24 where M is Ru, Rh or Ir) that have been prepared by calcination of HT precursors at 923 or 1173 K. The two techniques are complementary and are indispensable to the study of the oxide systems discussed herein. By using the two diffraction techniques, an investigation of the cation distribution in the different crystalline phases present in each sample has been carried out, focusing on the distribution of the noble metal. The preparation of samples having different Mg : Al ratios has allowed investigation of the role of the Mg : Al ratio and noble metal distribution on the catalyst activity in the partial oxidation of methane at low residence times.

Experimental

Sample preparation and characterisation

The samples were obtained from the HT precursors by calcination at 923 or 1173 K for 14 h. The HT precursors were prepared from the precipitation of a solution containing nitrate salts of M, Mg^{2+}, Al^{3+} (where M is Ru^{3+}, Rh^{3+} or Ir^{3+}), with a second solution containing a slight excess of Na_2CO_3. The pH was maintained at 10.0 by the dropwise addition of NaOH. The precipitates were kept in suspension at 333 K for 40 min and then filtered, washed [until the sodium content (as Na_2O) was lower than 0.02% w/w], and dried overnight at 363 K. The precursor compositions were determined after dissolution in concentrated HCl using complexometric titrations for aluminium and magnesium and spectrophotometric evaluation of the coloured complexes for the noble metals.[14–16]

---

†Basis of a presentation given at Materials Discussion No. 5, 22–25 September 2002, Madrid, Spain.

DOI: 10.1039/b205146j

The surface areas were determined by N_2 absorption using a Carlo Erba Sorpty model 1700.

Thermogravimetric analysis (TGA) was carried out using a TA instrument (TGA 2050) with a temperature ramp from 350 to 1173 K at a rate of 10 ° min^{-1}.

Data collection

Samples containing $M:Mg^{2+}:Al^{3+}$ ratios of 5 : 71 : 24 (where M is Ru^{3+}, Rh^{3+} or Ir^{3+}) were analysed by X-ray diffraction (XRD) and neutron diffraction. XRD powder data collection were obtained using copper radiation (λ = 1.5418 Å) and a Philips PW1050/81 diffractometer equipped with a graphite monochromator in the diffracted beam and controlled by a PW1710 unit. A 2θ range of 16–135° was investigated using a step size of 0.05° and a counting time of 22 s $step^{-1}$. After recording of the X-ray data, the samples were preserved under a nitrogen atmosphere for the neutron experiments.

Neutron diffraction experiments were performed on the D2B diffractometer at the ILL-High Flux Reactor in Grenoble using a wavelength of 1.594 Å [from the Ge (3 3 5) reflection] at a resolution $\Delta d/d$ of 5×10^{-4}.[17] An angular coverage of $5° < 2\theta < 162.5°$ for scans performed at step sizes of 0.05° were used. Scans were recorded at room temperature for samples contained in vanadium sample holders. Five scans (corresponding to a total of 750 000 neutron counts) were added to give the final profile of each sample.

Data analysis

Full pattern refinements based on the Rietveld method were carried out using the PC version of the DBWS-9807 program by Wiles and Young.[18–20] The content and location of the transition metal atoms were determined by performing a first batch of refinements using X-ray data. The structural data obtained were then used as the starting input file for a second batch of refinements on the neutron data. The M/(Mg + Al) ratios were kept fixed at the values obtained at the end of the first batch of refinements while all the other parameters where progressively varied in order to obtain a final result comprising the Mg and Al content of each metal site.

The X-ray and neutron cross sections of Ru, Rh, Ir, Al, Mg and O atoms were used.[21] Since Rh and Ir are quite significant absorbers of neutrons, no absorption correction was applied in the calculation of the background, but a fourth order polynomial equation was employed to calculate it while the peaks were fitted with a pseudo-Voigt function. One or two spinel-type phases (space group F*d*3*m*) were used to fit the mixed oxide phases (as mentioned in the Discussion) as well as an IrO_2 or RuO_2 phase (space group P4$_2$/*mnm*) where necessary.

The main features of each refinement batch were as follows. In the first cycle the scale factor and the background coefficients were refined. Successively, the profile parameters (peak widths and their dependence in 2θ, true 2θ zero, Lorentianity fraction) and the lattice parameters were also allowed to vary. Finally the occupancy factors (O.F.) were refined and cation substitution tested. The temperature factors (t.f.) in the form of isotropic B were fixed at the values determined from single crystal data of MgO[22] because of the former's strong correlation with the O.F. The same t.f. values were used for different chemical species occupying the same location. Only at the end of the refinement procedures, a small number of trials using t.f. values varied by 50% were carried out to assess the uncertainty in the O.F. due to possible inconsistencies in the t.f. In all cases the variations induced in the O.F. from variation of the t.f. were minor or equal to the O.F. estimated standard deviations (e.s.d.). The overall temperature parameter was refined for each phase. Different Fourier maps were used to verify the presence of cations in the 16c, 8a, 8b sites and to test the residual neutron density.

Further details of the crystal-structure investigations may be obtained from the Fachinformationszentrum Karlsruhe, D-76344 Eggenstein-Leopoldshafen, Germany on quoting the depository numbers from 411367 to 411375.

Catalytic tests

After activation at 750 °C for 5 h in a N_2/H_2 equimolar flow (7 l h^{-1}), the calcined samples reported later in Table 5 were tested in the partial oxidation of methane. The catalytic tests were carried on in a quartz reactor using an oven heated at 500 °C, feeding a gas mixture $CH_4:O_2:He$ = 2 : 1 : 4 and 2 : 1 : 20 v/v. The quartz reactor had an internal diameter of 6 mm and was filled with 0.075 g of catalyst in order to obtain a residence time of 7 ms. The reaction products were analysed on-line, after water condensation, by two gas chromatographs equipped with HWD and carbosieve SII columns, with He as the carrier gas for the analysis of CH_4, O_2, CO and CO_2, and N_2 as the carrier gas for the H_2 analysis.

Results and discussion

The materials obtained using the described preparation method were characterised by only a crystalline phase corresponding to an hydrotalcite like precursor.[10] The stability of the HT precursor was not affected by the insertion of Rh, Ru or Ir into the HT phase since TGA results showed the typical two weight loss features of the HT corresponding to interlayer water loss (430–460 K) and the contemporary evolution of H_2O from the cationic layer and CO_2 from the interlayer (650–690 K).

Rietveld analysis

Crystalline phases resulting from the thermal treatment of HT precursors at 923 or 1173 K and deduced from a comparison between X-ray and neutron patterns with ICDD files[23] are reported in Tables 1 and 2. Utilisation of the two complementary techniques is justified by the fact that: (i) determination of the occupancy factors of Mg and Al atoms from X-ray data is hindered by the closeness of the X-ray scattering lengths of both elements while the two have significantly different neutron scattering lengths, *b* (*b* values for Mg, Al, Ru, Rh, Ir are 0.52, 0.345, 0.73, 0.59, 1.06×10^{-12} cm, respectively);[21] and (ii) only the enormous differences between the X-ray scattering lengths of the transition metals investigated herein and those of Mg and Al atoms allow refinement of data based on the siting of a small percentage of the heavier metal.

After pre-treatment at 923 K, the major phases detected for the samples are a cubic mixed-oxide MgO-phase along with segregated MO_2 (M = Ir or Ru). For the samples preheated at 1173 K, a cubic, spinel-type oxide phase is observed along with the phases detected for the '923 K' sample. Surprisingly, a separate Rh-phase is not observed for any of the Rh-samples.

The location and amount of the transition metals were obtained from the full pattern refinement of both X-ray and neutron data. Since the MgO-type phase obtained from the HT precursor has been reported to be far from ideal,[11–13] a more flexible, spinel-like structure was adopted to model the MgO-type phase.

For sake of clarity it has to be taken into account that we use here the term 'MgO-type' phase to identify the phases whose diffraction patterns are very similar to that reported for MgO,[23] irrespective of the real structure that is reported in the data shown in the tables.

MgO and stoichiometric spinel have the same framework of oxygen atoms which differs essentially in two respects: (i) the '*a*' unit cell parameter of the spinel cell axis is almost twice that of the oxide one (8.083 Å for $MgAl_2O_4$ compared with 4.213 Å for MgO);[23] and (ii) the location of the cations and the degree of filling of the cavities defined by the oxygen atoms vary. In the

Table 1 The detected phases, refined structural parameters and agreement indexes R_p, R_{wp} for the samples M/Mg/Al 5 : 71 : 24 a.r. (atomic ratio) obtained from HT calcined at 923 K (e.s.d. in parentheses)

923 K	Rh			Ir			Ru		
Detected phases[a]	MgO			MgO + IrO_2			MgO + RuO_2		
MgO phase									
a/Å[b]	8.3833(8)			8.3987(7)			8.3855(6)		
x[c]	0.2496(5)			0.2499(8)			0.2495(5)		
Position[d]	16c	16d	8a	16c	16d	8a	16c	16d	8a
O.F.(Mg)	0.80(3)	0.26(5)	0.27(2)	0.73(4)	0.34(2)	0.29(2)	0.80(3)	0.30(2)	0.27(3)
O.F.(Al)		0.42(3)			0.44(7)			0.42(3)	
O.F.(M)		0.091(6)			0.074(5)			0.058(5)	
Proposed chemical formula[e]	$Mg_{0.60}Al_{0.21}Rh_{0.047}O$			$Mg_{0.61}Al_{0.22}Ir_{0.037}O$			$Mg_{0.62}Al_{0.21}Ru_{0.031}O$		
R_p	2.1			2.5			2.2		
R_{wp}	2.6			3.1			2.7		

[a] MgO = MgO-type phase. [b] Refined value relative to the mixed oxide supercell (spinel-type cell). Divide by 2 in order to compare with the MgO lattice type. [c] Oxygen fractional co-ordinate. [d] Cation presence was tested also in the 8b site but the O.F. were so close to zero that this site was considered empty in the final cycles. The O.F. are normalised to unity. M = Rh or Ir or Ru. [e] In the unit cell are contained 32 formula units.

spinel unit cell there are 32 oxygen atoms defining 32 octahedral and 64 tetrahedral interstices. In a stoichiometric $MgAl_2O_4$ spinel, only an eighth of the tetrahedral (crystallographic site 8a) and half of the octahedral cavities (site 16d) are occupied.[24–26] Therefore the spinel structure has many empty sites in which many ions can be accommodated.

The MgO unit cell (space group F$m\bar{3}m$ no. 225) contains four oxygen atoms and four crystallographically equivalent metal atoms co-ordinated octahedrally giving rise to the so-called 'rock-salt'-type structure. This lattice can be described using a supercell with a lattice parameter twice that of the oxide and the scaled down co-ordinates reported for the stoichiometric spinel space group, F$d\bar{3}m$ (no. 227).[25,26] The volume of the oxide supercell is eight-fold that of the original cell and contains 32 oxygen atoms and 32 cations that fill all the octahedrally co-ordinated positions. Owing to the F$d\bar{3}m$ space group symmetry rules,[27] the octahedral sites are non-equivalent and are identified as 16c and 16d. In a stoichiometric $MgAl_2O_4$, Al atoms occupy the 16d site, the 16c site is empty, while the Mg atoms occupy the tetrahedrally co-ordinated positions (site 8a). The last of these sites is empty in a 'rock-salt' structure like MgO. In other spinels, the distribution of the cations in the cavities may be different.[28–30] Non-stoichiometric spinels show structures intermediate between the spinel and 'rock-salt' types.[11–13]

In the refinement procedures for both X-ray and neutron diffraction experiments, a spinel structure was used in order to fit the MgO-type phase. For this reason, the refinement of the samples obtained by calcination at 1173 K was conducted using two spinel structures that had different unit cell parameters. The possibility of having cations in the octahedral 16c, 16d and tetrahedral 8a, 8b sites was verified.

Two typical X-ray patterns are shown in Fig. 1 and the final neutron data plots for all of the samples in Fig. 2. The distribution of the metal cations inside the different crystallographic positions derived from the refinements is reported in

Table 2 The detected phases, refined structural parameters and agreement indexes R_p, R_{wp} for the samples M/Mg/Al 5 : 71 : 24 a.r. obtained from HT calcined at 1173 K (e.s.d. in parentheses)

1173 K	Rh			Ir			Ru		
Detected phases[a]	MgO + S			MgO + IrO_2 + S			MgO + RuO_2 + S		
MgO phase									
a/Å[b]	8.4212(3)			8.4193(3)			8.4182(4)		
x[c]	0.2526(3)			0.2462(2)			0.2463(2)		
Position[d]	16c	16d	8a	16c	16d	8a	16c	16d	8a
O.F.(Mg)	0.92(4)	0.47(3)	0.16(3)	0.76(4)	0.71(5)	0.14(2)	0.78(2)	0.85(4)	0.097(4)
O.F.(Al)		0.26(3)			0.25(5)			0.11(5)	0.071(3)
O.F.(M)		0.076(6)			0.04(2)			0.026(5)	
Proposed[e] chemical formula	$Mg_{0.73}Al_{0.13}Rh_{0.038}O$			$Mg_{0.77}Al_{0.13}Ir_{0.020}O$			$Mg_{0.84}Al_{0.073}Ru_{0.013}O$		
Spinel phase									
a/Å[b]	8.1379(4)			8.1483(8)			8.1022(6)		
x[c]	0.2604(3)			0.2585(3)			0.2586(3)		
Position[d]	16c	16d	8a	16c	16d	8a	16c	16d	8a
O.F.(Mg)		0.11(2)	1.00(3)		0.131(9)	0.61(5)		0.23(4)	0.78(7)
O.F.(Al)		0.77(3)			0.818(5)	0.38(5)		0.77(4)	0.22(7)
O.F.(M)		0.112(5)			0.060(4)				
Proposed[e] chemical formula	$Mg_{1.3}Al_{1.6}Rh_{0.224}O_4$			$Mg_{0.87}Al_{2.00}Ir_{0.12}O_4$			$Mg_{1.25}Al_{1.77}O_4$		
R_p	2.4			2.8			2.8		
R_{wp}	3.0			3.5			3.5		

[a] MgO = MgO-type phase; S = cubic spinel-type phase. [b] Refined value relative to the mixed oxide supercell (spinel-type cell). Divide by 2 in order to compare with the MgO lattice type. [c] Oxygen fractional co-ordinate. [d] Cation presence was tested also in the 8b site but the O.F. were so close to zero that this site was considered empty in the final cycles. The O.F. are normalised to unity. M = Rh or Ir or Ru. [e] In the unit cell are contained 32 formula units indicated for the MgO-type phase and 8 for those of the spinel-type phase.

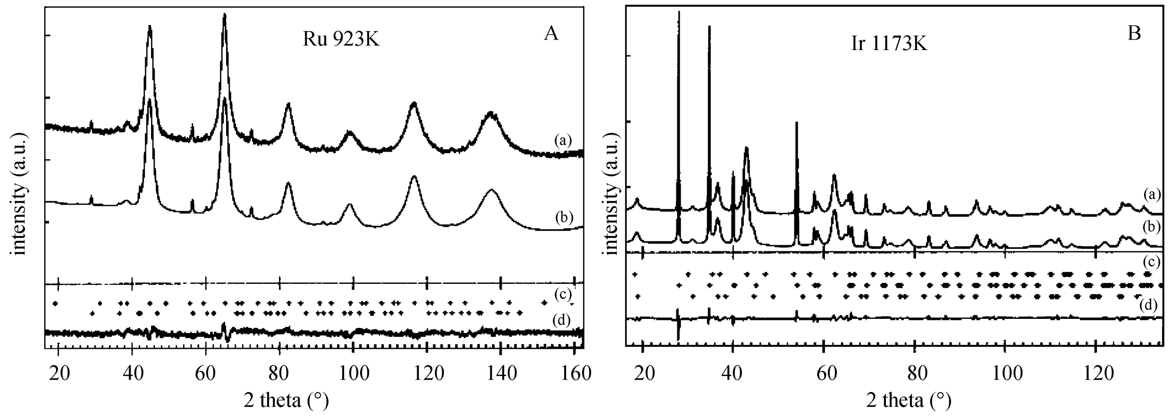

Fig. 1 As an example are reported (A) neutron refining of the Ru/Mg/Al 5 : 71 : 24 sample calcined at 973 K, and (B) X-ray diffraction profiles of the Ir/Mg/Al 5 : 71 : 24 sample calcined at 1023 K, both showing (a) the observed and (b) calculated patterns, (c) reflection position markers and (d) difference profile.

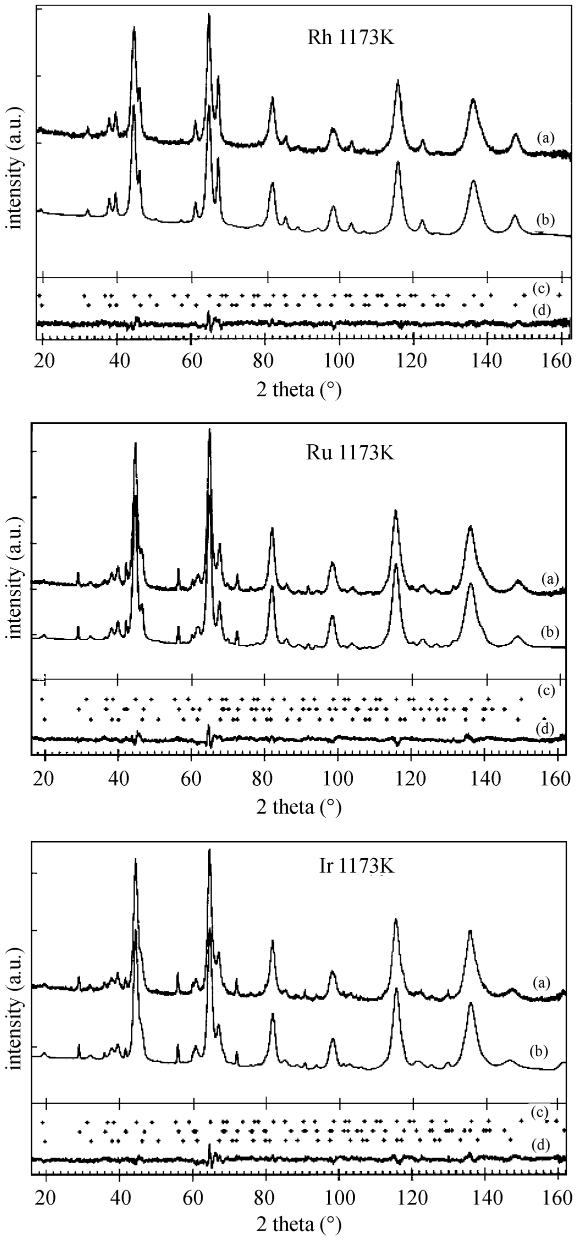

Fig. 2 Comparison between (a) the observed and (b) the calculated neutron powder patterns, (c) reflection position markers, and (d) difference profile of the sample M/Mg/Al 5 : 71 : 24 a.r. (M = Rh, Ru or Ir) calcined at 1173 K.

Tables 1 and 2 and the relative percentage distribution in Table 3. It is evident that the presence of Rh, Ir and Ru atoms exclusively in the 16d crystallographic site for MgO- and/or spinel-type phases occurs irrespective of the calcination temperature. Furthermore, the distribution of the cations reveals that the structures obtained by HT calcination are far from ideal. In particular, the MgO-type phases obtained by calcination of each sample at the two different temperatures are quite different: (i) for the samples calcined at 923 K, Mg atoms are distributed over 16c, 16d and 8a sites, while aluminium is found in 16d sites; (ii) the samples calcined at 1173 K show a lower aluminium content, a lower occupancy of the 8a sites and a further filling of the 16d sites. The segregation of the spinel phase leads to a rearrangement of the Mg/Al atoms inside the MgO-type phases at 1173 K, which show a distribution closer to a 'rock-salt' with respect to the 923 K samples.

The presence of a small amount of amorphous component in the samples, and the fraction of grain boundary material (evidenced by the relative high values for the surface area[10]), should be taken into consideration to explain some minor discrepancies arising from the comparison between the overall atom content, as deduced from the refinements, and the bulk chemical analyses. Nevertheless, the results obtained from cation analyses for all the samples are within the standard deviation of the O.F. calculated from the Rietveld analyses.

The amount of the transition metal inside MgO-type and spinel-type phases in the samples calcined at 923 and 1173 K decreases in the order Rh > Ir > Ru confirming their different solubilities in the two phases.

The unit cell parameters (Tables 1 and 2) show trends consistent with the amount of transition metal found inside the crystalline phases. Because of the structural consideration reported above the values of the a parameter for the MgO-type lattice must be compared with twice that of MgO (a = 4.213 Å, *i.e.* 8.426 Å).[23] Rh^{3+}, Ru^{3+} and Ir^{3+} each have a larger radius (0.66, 0.68 and 0.68 Å, respectively) than that of Al^{3+} (0.53 Å).[31] An enlargement of the unit cells can, therefore, be expected. Conversely, all of the values refined for the MgO-type cell reveal that indeed the cells are smaller, which is further evidence of a partial evolution of the system towards a spinel-like structure (a = 8.085 Å[26] for a stoichiometric Mg/Al spinel).

Among the factors that affect the value of the cell parameters, the most significant is the dimension of the 'host' ion. According to this it is possible to account for the increase of the a cell parameter for rhodium and iridium spinel-type phases (8.138 and 8.148 Å, respectively) in relation to that of the stoichiometric Mg/Al spinel. The parameter value for the

Table 3 Phase composition and distribution of the cations between the different crystalline phases obtained from HT calcination. (e.s.d. 2% of the values)

	923 K			1173 K		
	Rh	Ir	Ru	Rh	Ir	Ru
MgO–MO_2–S (%wt)[a]	100–0–0	98–2–0	94–6–0	69–0–31	61–11–28	66–10–24
Spinel fraction[b]	—	—	—	32	32	29
MO_2/MO_{2max} (%wt)[c]	0	11	40	0	50	71
M_{MgO}–M_{MO_2}–M_{spin} (atom%)[d]	0–100	11–89	38–62	59–0–41	30–49–21	22–78–0

[a] MgO = MgO-type phase; S = spinel-type phase; M = Rh or Ir or Ru. [b] Ratio between the spinel and the total mixed oxides: S/(MgO + S) as mol%. [c] Ratio between the amount of the segregated MO_2 and its maximum segregable amount. [d] Distribution % of the transition metal atoms between the two (923 K) or three phases (1173 K).

iridium sample is only marginally larger than that of the rhodium sample because of its limited presence into the lattice (O.F. values for the 16d position in the spinel phase are 0.06 and 0.11 for iridium and rhodium samples, respectively). The spinel-type phase obtained from the ruthenium sample calcined at 1173 K has a cell parameter *a* of 8.102 Å (which is close that of the stoichiometric spinel) confirming the absence of any appreciable amount of ruthenium in the spinel.

As can be deduced from Table 3 data, the Rh atoms are fully dissolved inside the mixed oxide phases while Ir and Ru atoms segregate to minor quantities of IrO_2 and RuO_2. For the samples calcined at 923 K, the transition elements show good solubility in the MgO-type phase: 100, 89 and 62 atom% for Rh, Ir and Ru, respectively. The solubility of the transition elements in the mixed oxides obtained after calcination at 1173 K is reduced in fact, the overall atom% found in the MgO- and spinel-type oxides is 51 and 22, for iridium and ruthenium, respectively. The total solubility of rhodium remains at 100 atom%.

Different attributes of the transition metals in the three crystalline phases of the samples obtained after calcination at 1173 K are revealed: (i) Rh atoms are found in MgO- and spinel-type phase; (ii) Ru atoms are distributed over the MgO-type phase and the segregated RuO_2; and (iii) Ir atoms are distributed over the three phases. The quantities of transition metal inside the MgO-type and spinel phases vary as Rh > Ir > Ru a trend which varies inversely to the amounts of segregated MO_2 (M is Ir or Ru). The quantities of the segregated oxide are related to the global thermal stability of the mixed oxides. The latter is a function of the chemical nature of the dissolved element, and the following order of thermal stability Rh > Ir > Ru is confirmed.[10] The order is a reverse of the stability of the trivalent oxides.[32]

The atom% distribution shown in Table 3 is the product of the proportion of the element substitution in a particular phase and the amount of the phase in the sample. For this reason it should be noted that for rhodium samples calcined at 1173 K, the rhodium is distributed at 41 atom% in the spinel and 59 atom% in the MgO-type phase. Nevertheless, the solubility of the transition element in the spinel-type phase is still considerably higher than in the MgO-type oxide (the spinel phase being 31 wt% of the entire sample). The iridium solubility between the two mixed oxides is observed to behave similarly but the main part of the transition element is contained in the segregated IrO_2 phase. The ratio of Rh or Ir atoms between the MgO- and the spinel-type phases is almost constant at 1.4. Ru atoms are located for most part in the segregated phase and do not show any solubility in the spinel phase.

Characterisation of samples having different Mg : Al

The different solubilities of the transition elements in the two mixed oxides suggest that their presence is a useful tool for controlling the relative amount of the different oxide phases. The variation of the $M^{2+}:M^{3+}$ ratio may be considered as a practical way of controlling the relative amount of the transition metal inside the mixed oxides, and *vice-versa*.

On this basis, two Rh samples at the limit of the HT composition range in terms of $M^{2+}:M^{3+}$ were prepared in order to search for the relation between the Rh position and the activity in the partial oxidation of methane (Table 4). XRD analysis of the precursors shows that for the whole series only the HT phase is present (Fig. 3). The changes in the lattice parameters are consistent with the variation of the Mg : Al ratio: the *a* parameter increases with the Mg content, due to its larger cationic radius; and the *c* parameter decreases with the

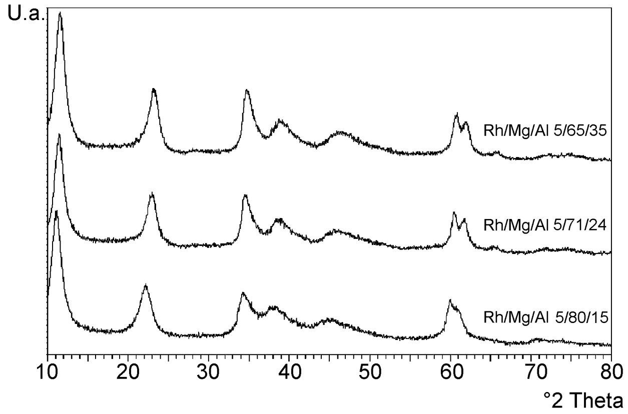

Fig. 3 XRD analysis of the Rh/Mg/Al-HT precursors having different Mg : Al ratios.

Table 4 Composition lattice parameters and surface area of the Rh and Ru samples prepared with different $M^{2+}:M^{3+}$ ratios

Sample	Composition as atomic ratio	Precursor (HT)		Sample calcined at 1173 K		Surface area
		a/Å	*c*/Å	MgO-type *a*/Å	Spinel *a*/Å	Calcined/$m^2\ g^{-1}$
Rh/Mg/Al	5 : 80 : 15	3.085(4)	24.04(3)	8.422(2)	Not present	96
Rh/Mg/Al	5 : 71 : 24	3.075(3)	23.34(1)	8.421(1)	8.138(1)	91
Rh/Mg/Al	5 : 65 : 30	3.052(3)	23.14(2)	8.422(3)	8.120(3)	88
Ru/Mg/Al	1 : 80 : 19	3.079(3)	23.90(2)	8.419(2)	8.090(4)	82
Ru/Mg/Al	1 : 71 : 28	3.072(4)	23.13(2)	8.424(2)	8.102(2)	97

Table 5 Relative amount of the MgO and spinel phases and Rh distribution between the phases in the Rh/Mg/Al samples

Rh/Mg/Al	5 : 80 : 15	5 : 71 : 24	5 : 65 : 30
MgO–S (%wt)[a]	100–0	69–31	65–35
Rh_{MgO}–Rh_{spin} (atom%)	100–0	59–41	43–57

[a] MgO = MgO-type phase; S = spinel-type phase.

increase of the Al content due to the increase of the charge density and of the interaction between layer and interlayer.

The two samples having the composition Rh/Mg/Al of 5 : 80 : 15 and 5 : 65 : 30 as atomic ratio calcined at 1173 K have been analysed by XRD analysis in order to determine the Rh position in the calcined materials. The XRD of the Rh/Mg/Al 5 : 65 : 30 was refined by Rietveld analysis using the model previously described. The analysis was carried out to determine the relative amount of the two phases and the relative Rh distribution (Table 5). The increase of the amount of the spinel phase with respect to the Rh/Mg/Al 5 : 71 : 24 is consistent with the increase of the Al content; at the same time the percentage of the Rh in the spinel increases (O.F. of Rh in the 16d sites is 0.148 with respect to the 0.112 of the sample Rh/Mg/Al 5 : 71 : 24). As a result, the Rh content inside the spinel structure is 57% of the total amount, confirming that the variation of the Mg : Al ratio is a good system to change the Rh distribution. XRD analysis of the Rh/Mg/Al 5 : 80 : 15 sample calcined at 1173 K confirms this trend, showing only the MgO-type phase without any presence of the spinel-phase (Fig. 4). Therefore in this case the Rh is completely soluted in the MgO-phase together with the Al. The results confirm the Rietveld analysis of the Rh/Mg/Al 5 : 71 : 24 sample in which was found the presence of a significant amount of Rh and Al soluted in the MgO-phase; furthermore, it is also clear that at low M^{3+} content (Al and Rh) it is possible to trap the M^{3+} cation in the MgO phase even after calcination at high temperature.

Rietveld analysis of the XRD and neutron combined data carried out on the Ru/Mg/Al 5 : 71 : 24 as atomic ratio has shown a large amount of segregated phase and the presence of the Ru in the oxide phase. This result was utilised to prepare two samples containing 1% of Ru (Ru/Mg/Al 1 : 80 : 19 and 1 : 71 : 28 as atomic ratio) with the aim of minimising the segregated Ru (Table 4). The amount of Ru was decreased in order to facilitate the comparison in the characterisation and in the activity during the partial oxidation of methane, which can be complicated by a large amount of the segregated RuO_2 phase. XRD analysis of the sample confirms the presence of only the HT phase.

XRD of the Ru samples calcined at 1173 K (Fig. 4) was analysed in terms of RuO_2 segregation. In the Ru/Mg/Al 1 : 71 : 28 sample the RuO_2 is 50% of the total Ru,[10] while only traces of RuO_2 are present in the Ru/Mg/Al 1 : 80 : 19 sample. These results on the proportion of RuO_2 confirm the distribution of Ru between the RuO_2 and MgO phases that has been found with the Rietveld analysis. Also in this case the importance of the Mg : Al ratio in the Ru distribution between the phases is clear since an increase of the MgO phase allows the insertion of a higher amount of Ru in this phase and a decrease of the RuO_2 amount. The presence of the spinel phase in the Ru sample of $M^{2+} : M^{3+}$ = 80 : 20 a.r. (Ru/Mg/Al 1 : 80 : 19) is probably due to the lower solubility of the Al with respect to Rh (Rh/Mg/Al 5 : 80 : 15) in the MgO phase and to the segregation of a small amount of RuO_2 which helps the rearrangement of the structure.

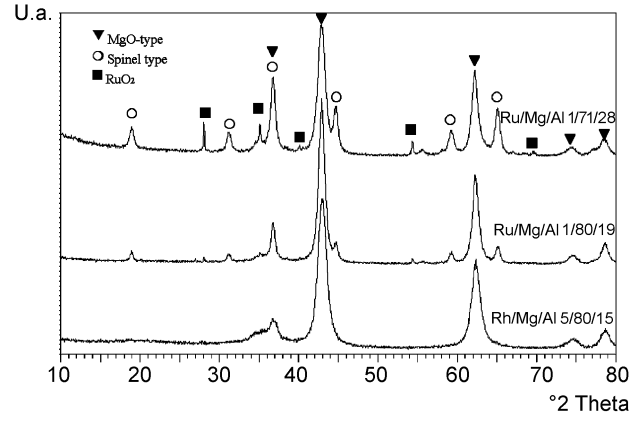

Fig. 4 XRD analysis of the Rh/Mg/Al 5 : 80 : 15, Ru/Mg/Al 1 : 80 : 19 and 1 : 71 : 28 samples calcined at 1173 K.

The calcined samples were characterised in terms of surface area before the catalytic tests. All samples show a very high surface area (ranging between 80 and 100 $m^2\ g^{-1}$) without an evident effect of variation in the $M^{2+} : M^{3+}$ ratio. The high surface area highlights the good thermal stability of these samples and allows a good dispersion of the metal also with high metal loading. The surface area of the catalysts does not change after the tests in the partial oxidation of methane, confirming the stability of these materials.

Catalytic test on the partial oxidation of methane

The three Rh samples were tested, after reduction *in situ*, in the partial oxidation of methane at low residence time under two different sets of conditions: $CH_4 : O_2 : He$ = 2 : 1 : 4 with a reaction mixture close to that of an industrial process mimics the use of air as oxidising feed; and a 2 : 1 : 20 v/v composition in order to enhance the differences among the catalysts. Both sets of conditions were used in order to correlate the Rh position in the calcined samples with the catalytic activity.

In the tests carried out, feeding a concentrated gas mixture at a residence time of 7 ms with an oven temperature of 773 K, the maximum temperature measured by the thermocouple was close to 973 K because of the presence of highly exothermic oxidation reactions. All of the catalysts show total oxygen conversion, high methane conversion, and synthesis gas selectivity close to 90% (Fig. 5A). The catalytic results obtained under these conditions show significant differences between the

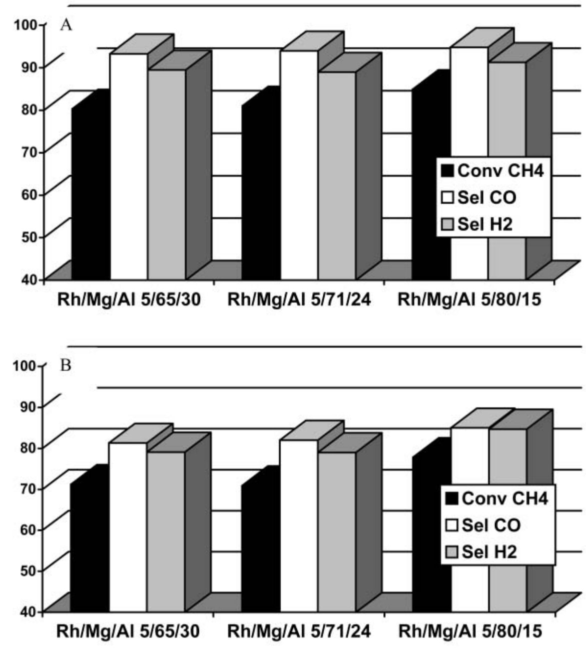

Fig. 5 Comparison of the activity of the Rh/Mg/Al catalysts containing 5% Rh (a.r.) in the partial oxidation of methane carried out at a residence time of 7 ms with an oven temperature of 773 K: (A) $CH_4 : O_2 : He$ 2 : 1 : 4 v/v; (B) $CH_4 : O_2 : He$ 2 : 1 : 20 v/v.

sample Rh/Mg/Al 5 : 80 : 15 and the two sample Rh/Mg/Al 5 : 71 : 24 and 5 : 65 : 30. In particular, the sample in which only the MgO-type phase is present (Rh/Mg/Al 5 : 80 : 15) has a higher methane conversion and synthesis gas selectivity in comparison with the samples in which the MgO and spinel phases are present, while the difference between these two samples was not significant.

The large amount of heat produced during the reaction may affect the thermal profile and surface temperature of the catalysts which have a strong influence on methane conversion and syngas selectivity.[33] Therefore, catalytic tests using diluted gas mixtures were carried out to reduce the heat production and the thermal effect of the exothermic reactions, improving the significance of the comparison.

During the diluted tests ($CH_4 : O_2 : He = 2 : 1 : 20$ v/v) carried out at 773 K the catalysts showed, besides total oxygen conversion, lower methane conversion and syngas selectivity (Fig. 5B) due to the lower temperature measured under there conditions (the maximum temperature measured was 890 K). As a consequence, the differences among the catalysts were enhanced, and the catalyst characterised by the presence of only the MgO-type phase was much more active than the catalysts characterised by the presence of spinel- and MgO-type phases. These results can be explained on the basis of the specific activity of the Rh supported and intimately mixed with the MgO which has a positive effect.[34] On the other hand, the catalytic activities of the two other samples are very similar since the differences in the Rh distribution are not very marked and the amount of Rh in each phase in both catalysts is still very high.

Analogous conditions were also used to compare the Ru catalysts. The activity of the Ru catalysts is lower than those containing Rh because of the lower amount of active phase and the lower specific activity of Ru. The comparison carried out at 773 K in diluted conditions ($CH_4 : O_2 : He = 2 : 1 : 20$ v/v) between the two Ru samples showed (Fig. 6) a high activity of the sample having the majority of the Ru soluted in the MgO phase, while the activity of the sample having a large proportion of the Ru segregated as RuO_2 is low due to the low dispersion of the Ru. The differences confirm the importance of the dispersion of the metal and the interest of the methodology based on the solubility of the cation in an inert matrix.

Conclusions

A flexible preparation method, involving the insertion of the active phase in the cationic layer of a hydrotalcite-type precursor, has been applied for the preparation of high temperature Rh, Ru and Ir catalysts.

The mixed oxide structures obtained after calcination at 923 K of M/Mg/Al 5 : 71 : 24 have been refined by Rietveld analysis of XRD and neutron diffraction data to characterise the materials fully. The combined analysis clearly evidences the formation of an MgO phase far from the ideal rock salt structure, with a relevant fraction of Mg in the tetrahedral position. The Rh shows complete solubility in this phase, while the solubility of Ru and Ir is high but not complete.

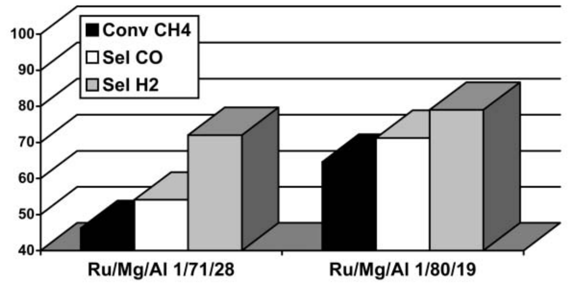

Fig. 6 Comparison of the activity of the Ru/Mg/Al catalysts containing 1% Ru (a.r.) in the partial oxidation of methane carried out at a residence time of 7 ms with an oven temperature of 773 K using a diluted gas mixture ($CH_4 : O_2 : He$ 2 : 1 : 20 v/v).

The increase of the calcination temperature (1173 K) has shown the expected rearrangement of the mixed oxide structure leading to a more ideal MgO-type structure, a spinel structure and an MO_2 phase (for Ir and Ru). The solubility of the transition metals inside the MgO-type and the spinel-type phases has been found to be highest for rhodium (which did not segregate even after calcination at 1173 K) and lowest for ruthenium atoms, a trend which varies inversely with the amount of segregated MO_2. Moreover, the transition metals show a different distribution in the three crystalline phases of the samples: (i) Ir atoms are distributed over the three phases; (ii) Ru atoms are distributed over the MgO-type phase and the segregated RuO_2; and (iii) Rh atoms are found in MgO- and spinel-type phases in different concentrations.

The results of the refinement have allowed a breakthrough in the preparation of Rh, Ru and Ir catalysts since the different distributions of Rh, Ru and Ir in the phases enables the preparation of samples with different Mg : Al ratios, changing the relative abundance of the oxide phase and affecting the solubility and the distribution of the elements in the materials obtained after calcination at 1173 K.

The presence of different concentrations of Rh in the two phases allows modification of the Rh distribution by changing the Mg : Al ratio. A decrease of the Mg : Al allows retention of more than 50% of Rh in the spinel phase, whereas the sample Rh/Mg/Al 5 : 80 : 15 a.r. after calcination at 1173 K exhibits only the MgO-type phase with all Rh soluted in this phase. This catalyst, after reduction, shows very interesting catalytic performances in the partial oxidation of methane, showing a methane conversion and synthesis gas selectivity significantly higher than those of the samples with an analogous Rh loading but with lower Mg : Al ratios.

Because of the different solubility of Ru in the MgO and spinel phases it has also been possible to reduce its segregation by changing the Mg : Al ratio. The segregation of Ru decreases with an increase of the MgO phase leading to an increase of the catalytic activity.

Acknowledgements

The authors wish to thank Dr Emmanuelle Suard and Mr Peter Cross (ILL, Grenoble) for scientific and technical support during the experiments and ILL for beam time allocation. The financial support from Ministero per l‘Universita’ e la Ricerca Scientifica e Tecnologica and Consiglio Nazionale delle Ricerche (Italy) is gratefully acknowledged.

References

1 F. Cavani, F. Trifirò and A. Vaccari, *Catal. Today*, 1991, **11**, 173 and refs. cited therein.
2 F. Trifirò and A. Vaccari, in *Comprehensive Supramolecular Chemistry*, J. L. Atwood, J. E. D. Davies, D. D. Mc Nicol and F. Vögtle, ed., Pergamon, Oxford, 1996, vol. 7, ch. 8.
3 A. Vaccari, *Catal. Today*, 1998, **41**, 53.
4 F. Basile, L. Basini, G. Fornasari, M. Gazzano, F. Trifirò and A. Vaccari, *Chem. Commun.*, 1996, 2435.
5 F. Basile, L. Basini, G. Fornasari, M. Gazzano, F. Trifirò and A. Vaccari, in *Preparation of Catalysts VII*, B. Delmon, P. A. Jacobs, R. Maggi, J. A. Martens, P. Grange and G. Poncelet, ed., Elsevier, Amsterdam, 1998, pp. 31–40.
6 S. Y. Lee and R. Aris, *Catal. Rev. Sci. Eng.*, 1985, **27**, 207.
7 G. A. Foulds and J. A. Lapszewicz, in *Catalysis*, The Royal Society of Chemistry, Cambridge (UK), 1994, vol. 11, ch. 10.
8 D. A. Hickman, E. A. Haupfear and L. D. Schmidt, *Catal. Lett.*, 1993, **17**, 223.
9 M. Komiyama, *Catal. Rev. Sci. Eng.*, 1985, **27**, 341.

10 F. Basile, G. Fornasari, M. Gazzano and A. Vaccari, *Appl. Clay Sci.*, 2000, **16**, 185.

11 B. Rebours, J. B. d'Espinose de la Caillerie and O. Clause, *J. Am. Chem. Soc.*, 1994, **116**, 1707.

12 M. Gazzano, W. Kagunya, D. Matteuzzi and A. Vaccari, *J. Phys. Chem. B*, 1997, **101**, 4514.

13 M. Bellotto, B. Rebours, O. Clause, J. Lynch, D. Bazin and E. Elkaim, *J. Phys. Chem.*, 1996, **100**, 8535.

14 E. C. Cerceo and J. J. Markham, *Anal. Chem.*, 1966, **38**, 1426.

15 A. Vogel, *Textbook of Quantitative Inorganic Analysis*, Longman, London, 1978.

16 G. Charlot, *Chimie Analytique Quantitative*, Masson, Paris, 1974, pp. 490–494.

17 *Guide to Neutron Facilities at the ILL*, H. G. Buttner, E. Lelievre-Berna and F. Pinet, ed., Insitut Max Von Laue-Paul Langevin, Grenoble, December 1997.

18 H. M. Rietveld, *Acta Crystallogr.*, 1967, **22**, 151.

19 H. M. Rietveld, *J. Appl. Crystallogr.*, 1969, **2**, 65.

20 D. B. Wiles and R. A. Young, *J. Appl. Crystallogr.*, 1981, **14**, 149.

21 *International Tables for X-Ray Crystallography, Vol IV*, Kynoch Press, Birmingham, 1974.

22 S. Sasaki, K. Fujino and Y. Takeuchi, *Proc. Jpn. Acad.*, 1979, **55**, 43; reported as Inorganic Crystal Structure Database file no. 9863.

23 International Center for Diffraction Data, Newtown Square, PA, USA. File nos. 4-829 (MgO), 21-1152 ($MgAl_2O_4$), 43-1019 (IrO_2), 43-1027 (RuO_2).

24 A. F. Wells, in *Structural Inorganic Chemistry*, Oxford University Press, Oxford, 1984, pp. 592–596.

25 R. W. G. Wyckoff, in *Crystal Structures, Vol. 4*, Interscience Publishers, New York, 1968, pp. 76–79.

26 P. Fischer, *Z. Kristallogr.*, 1967, **124**, 275.

27 *International Tables for X-Ray Crystallography, Vol I*, Kynoch Press, Birmingham, 1974.

28 R. C. Peterson, G. A. Lager and R. L. Hitterman, *Am. Mineral.*, 1991, **76**, 1455.

29 W. L. Smith and A. D. Hobson, *Acta Crystallogr., Sect. B*, 1973, **29**, 362.

30 H. Berg, E. M. Kelder and J. O. Thomas, *J. Mater. Chem.*, 1999, **9**, 427.

31 R. D. Shannon, *Acta Crystallogr., Sect. A*, 1976, **32**, 751.

32 N. N. Greenwood and A. Earnshaw, *Chemistry of the Elements*, Pergamon, Oxford, 1989.

33 F. Basile, G. Fornasari, F. Trifirò and A. Vaccari, *Catal. Today*, 2001, **64**, 21.

34 E. Ruckenstein and H. Y. Wank, *Appl. Catal. A: General*, 2000, **198**, 33.